Role of quantum ion dynamics in the melting of lithium

S. F. Elatresh, S. A. Bonev, E. Gregoryanz, and N. W. Ashcroft

Phys. Rev. B **94**, 104107 — Published 9 September 2016

DOI: 10.1103/PhysRevB.94.104107

Role of quantum ion dynamics in the melting of lithium

S. F. Elatresh[1], S. A. Bonev[1,2*] and E. Gregoryanz[3], and N. W. Ashcroft[4]
[1]*Department of Physics, Dalhousie University, Halifax, Nova Scotia B3H 3J5, Canada.*
[2] *Lawrence Livermore National Laboratory, Livermore, California 94550, USA.*
[3]*SUPA, Centre for Science at Extreme Conditions and School of Physics and Astronomy, The University of Edinburgh, Edinburgh, EH9 3JZ, UK.*
[4]*Laboratory of Atomic and Solid State Physics, Cornell University, Ithaca, NY 14853, USA.*

The role of quantum ion dynamics in the low melting temperatures of Li is investigated from first principles theory. Free energies of solid and liquid phases are obtained at the classical and quantum ion levels. The results are used to determine the Li melting curve in the 40–60 and 110–150 GPa pressure ranges and are in excellent agreement with experimental data around 50 GPa. They predict the resumption of a positive melting slope at higher pressure. Quantum corrections to individual energy terms are far more significant than their net effect on the melting temperatures near 50 GPa, even though lithium behaves as a quantum solid at this pressure. The scales of these corrections increase with compression. A case is made for the possibility for anomalous melting at much higher pressures, where quantum ion dynamics are expected to play a prominent role.

PACS numbers: 62.50.-p,64.70.D-,65.40.-b

The phase diagram of Li has attracted considerable interest recently from both theory and experiment in relation to a number of counterintuitive electronic and structural changes observed under pressure. These include a deviation from simple metallic behavior, increasingly high temperature superconductivity, and a reentrant translation from metal to semiconductor [1–7]. One of the most remarkable properties of dense lithium is its anomalous melting. Despite numerous efforts, only recently has a clear experimental picture of the high pressure phase diagram and melting curve up to 75 GPa been established[8]. The anomalous melting behavior of Li was initially predicted based on the similarity between the high pressure crystalline phases of Na and Li. Tamblyn *et al.*[5] proposed that Li would undergo similar transitions to those found in liquid Na[9–12], thus leading to projections of anomalous melting of Li. They employed a "heat-until-melt" approach with molecular dynamics to compute melting temperatures up to 90 GPa. The melting curve was then predicted to have a minimum at about 65 GPa and 270 K[5]. A succeeding study using a two-phase simulation method found somewhat lower melting temperatures[13]. The turnover of the melting curve is at about the same pressure in both calculations.

Subsequent x-ray diffraction measurements[8,14] qualitatively confirmed the turnover of the melting curve, but also determined the minimum to be at lower temperatures than in the theoretical calculations. This raises the question of whether the quantum ion dynamics, which were not taken into account in the previous theoretical treatments [5,13], can account for the difference. Even though it was previously suggested that quantum corrections might play a significant role[8,15], no conclusive evidence of this effect has been provided up to date. Further, the recent work of Schaeffer *et al.*[16] who measured the melting curve using resistivity measurements found the melting minimum to be above 300 K, i.e. over 100 K higher than the results reported by Guillaume *et al.*[8].

The purposes of this article are therefore twofold. First, we seek to determine the role of quantum ion dynamics in the anomalous melting of Li. This is achieved by computing the free energies of both solid and liquid Li (i) first assuming classical ions, and then (ii) with corrections to account for quantum ion dynamics. The lowering of the melting temperature arising from quantum effects can thus be isolated. For this analysis we focus on the region between 40 and 60 GPa (about 2.8-fold compression compared to one atmosphere Li) where quantum effects are likely to be strongest and the relevant crystalline phase has the $cI16$ space group symmetry. The second of the goals is to provide an accurate theoretical value for the lowest melting temperature of the Li, as well as to extend its melting curve up to 150 GPa – a pressure region where the solid transforms to the lower symmetry $oC24$ structure and where no melting data are yet available.

To obtain the liquid phase Gibbs free energies and classical-ion enthalpies for the solid phase ($cI16$), we have carried out first principle molecular dynamic (FPMD) simulations of ^{7}Li for pressure from 38 to 65 GPa and temperatures up to 1000 K. We used finite-temperature density functional theory (DFT)[17] within the Perdew-Burke-Ernzerhof generalized gradient approximation (PBE-GGA)[18] as implemented in VASP[19]. The simulations were carried out in the canonical ensemble (NVT) using Born-Oppenheimer dynamics, with a Nosé-Hoover thermostat. Here N is the number of atoms, V is the volume and T is the temperature. These simulations were carried out with 128-atom supercells, 3-electron projector augmented wave pseudo-potential (PAW PP), and 340 eV plane-wave cut-off. For each density and temperature, the system was initially equilibrated within 1-2 ps and subsequently simulated for 10 ps or more using 0.75 fs ionic time-step (1/56 of the shortest phonon period). The plane-wave cut-off convergence was tested up to 400 eV for pressure at 45 GPa and temperatures 100, 400, and 3000K. The resulting convergence

of E and PV is within 1 meV/atom. In addition, convergence tests for finite size effects and **k**-point Brillouin zone sampling were performed at the above specified conditions. These included: (i) first principles molecular dynamics simulations (FPMD) simulations with 192-atoms supercells and the Γ **k**-point; (ii) FPMD simulations with 288-atoms supercells and the Γ **k**-point; and (iii) FPMD simulations with 128-atom supercells and a $2 \times 2 \times 2$ **k**-point grid. In all tests, the convergence of E and PV proved to be within one meV/atom.

Entropies of the classical and quantum harmonic solids, as well as enthalpies in the quantum ion case, are obtained by computing the phonon dispersions of Li in the $cI16$ phase. DFT perturbation theory[20] as employed in the ABINIT code[21] with Hartwigsen-Goedeker-Hutter PP's[22] and the PBE-GGA were used. A plane-wave expansion with a 2700 eV cut off and sufficiently dense **k**-point grids $12 \times 12 \times 12$ were used to ensure convergence of free energies better than 0.5 meV/atom. The dynamical matrices were computed on uniform **q**-point meshes, from which interatomic force constants were obtained and used to interpolate the phonon dispersions over the entire BZ's. The **q**-point grids were tested until convergence for the resulting Helmholtz free energies and entropy better than 0.5 meV/atom was achieved. For this a $5 \times 5 \times 5$ grid was required. To verify that anharmonicities can be neglected, the Helmholtz free energy of the $cI16$ crystal was calculated for 50 GPa and 300 K within the self-consistent ab initio lattice dynamics method (SCAILD) implemented in the SCPH package[23] . The result differs by only 0.33 meV/atom from the quasi-harmonic free energy at the same conditions.

Assuming classical ions, Gibbs free energies for liquid and solid phases were evaluated as $G = \langle E \rangle + \langle P \rangle V - TS$, where $\langle\rangle$ is a statistical average over the FPMD trajectories, E , P are the instantaneous total energy and pressure respectively, and S is the entropy. The classic ion internal energies are calculated from FPMD using $\langle E \rangle = \langle E_{DFT} \rangle + 3/2NKT$, with E_{DFT} being the DFT energy for a given atomic configuration, and $3/2NKT$ the ion kinetic energy. The pressure for solid and liquid phases is also obtained from the simulations as $P = -\frac{\partial E_{DFT}}{\partial V} + \frac{NkT}{V}$.

The entropy for the liquid was calculated using a reference entropy at $T_0 = 1000$ K obtained from previous work[24], and then integrating the specific heat, C_V, at a fixed volume to obtain the entropy at the desired T:

$$S(V,T) = S(V,T_0) + \int_{T_0}^{T} \frac{C_V}{T'} dT'. \qquad (1)$$

The integral is performed well by fitting C_V to a polynomial for the temperature range from 300 to 1000 K.

For the solid phase, the entropy was calculated at each volume of interest by integrating the phonon density of state, $g(\omega)$, assuming classical oscillators as $S_{cl} = 3Nk\left[1 - \int d\omega g(\omega) \ln(\hbar\omega/kT)\right]$.

The quantum corrections to the ionic free energies for the liquid were obtained based on the Wigner-Kirkwood

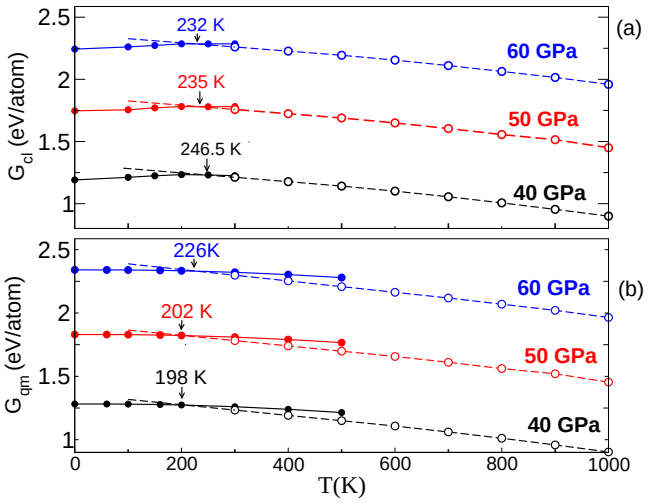

FIG. 1: Gibbs free energies for solid ($cI16$) and liquid lithium, represented by solid and dash lines, respectively. Results for classical ions are shown in (a) and for quantum ions in (b). The lines cross at the melting temperature for the given pressure.

approximation, which is known to be valid for systems not too far off from classical:

$$\Delta F_{qm} = \frac{h^2}{24k_B^2T^2} < \sum_i \frac{F_i^2}{m_i} >_{cl}, \qquad (2)$$

where the average is over the classical ensemble, and F_i and m_i are the ionic forces and masses.

Quantum corrections for the solid phase free energies were then evaluated by taking into account the phonon contributions to the free energy as $G = E_0 + P_0V + P_{ph}V + F_{ph}$, where E_0 and P_0 are the static lattice energy and pressure, P_{ph} and F_{ph} are the phonon pressure and free energy respectively. In all cases, E_0 and P_0 are taken from the VASP calculations in order to eliminate systematic differences between the static and MD simulations performed with the two different codes. The phonon Helmholtz free energy is $F_{ph} = U_{ph} - TS_{ph}$, and U_{ph} and S_{ph} are the phonon internal energy and entropy respectively. Here P_{ph} is calculated from $P_{ph} = -\frac{\partial F_{ph}}{\partial V} \mid_{N,T}$. For this purpose, F_{ph} is computed for several volumes and interpolated with a quadratic function of V.

Free energies for classical ions were determined for solid and liquid phases and then interpolated along each isotherm in order to compare their relative values along specific isobars (for further details see Supplementary Material). The final results for three isobars are shown in Fig. 1(a). The intersections of the solid and liquid Gibbs free energy curves give the respective melting temperatures. The same procedure was followed for determining the free energies but with quantum corrections, and the results are shown in Fig. 1(b).

Inclusion of quantum dynamics lowers the melting temperature. While the effect is noticeable, it is not

so dramatic as one might anticipate from considerations of the crystalline zero point energy alone. In order to make sense of this result, we have examined the relevant free energy terms. Their temperature dependences at 50 GPa are shown in Fig. 2. The quantum correction to the solid enthalpy ($\Delta H^s = H^s_{qm} - H^s_{cl}$) is indeed significant - larger than $\sim$ 56 meV/atom below 200 K, confirming that Li melts as a quantum solid at this pressure. However the effect of entropy is just the opposite, as it is lower for classical oscillators than for quantum counterparts by $\sim$ 17.5 meV/atom. Furthermore, the quantum nature of the liquid must be considered as well, and it contributes as much as $\sim$ 23 meV/atom at 200 K. When all free energy terms are considered, the difference between the quantum corrections to the solid and liquid Gibbs free energies, $\Delta G^s - \Delta G^l$, is only about $\sim$ 15.5 meV near the melting point, i.e. a third of ΔH^s.

It is interesting to compare these results with previous studies[25–31] of the isotope effect on the melting curves of the two lighter than Li elements, H and He. In general, there are several competing factors that determine the sign of the quantum correction to the melting curves: (i) The scaling of the kinetic energy with ion mass, $\propto 1/m^\alpha$, where α is 0.5 for a harmonic solid, but is generally > 0.5 for a liquid; (ii) Density differences between the two phases at coexistence; (iii) The collective lattice motion in the solid, keeping atoms more effectively away from their neighbors[28]; (iv) Structural differences. Previous studies[25–28] found that there is a large cancelation in the quantum corrections to liquid and solid He. A path integral Monte Carlo study[28] showed that at the same density, the liquid has higher kinetic energy due to (iii) above. However, the density of the solid is higher at co-existence and the net result is that the lighter He isotope has lower melting temperature[28]. An *ab initio* study[29] of H_2 and D_2 reported a change in the sign of the isotope (quantum) effect on the melting curve with pressure, most likely related to the onset of a gradual dissociation in the liquid. Interestingly, the computed isotope effect at low pressure in Ref. 29 is opposite to experimental measurements[30]; this could be an artifact of the crystal structures chosen to construct the free energy functions in Ref. 29. For monatomic metallic H at extreme compression (600-1600 GPa), Geng et al.[31] determined that the quantum effects lower the melting temperature by about 100-120 K. In the present case of Li, the solid and liquid densities are identical at coexistence near 50 GPa, and the two phases have similar local structural environments[5]. The larger quantum corrections in solid compared to liquid Li mean that (i) is the dominating factor here. At pressure above 50 GPa, where the melting slope is positive, the density differential (based on the Clapeyron equation) will play an additional role in favor of larger quantum corrections in the solid phase.

Our final results for the melting temperatures of the $cI16$ phase for quantum and classical ion dynamics are shown in Fig. 3. The agreement of the quantum results with the recent experimental measurements[8] is indeed ex-

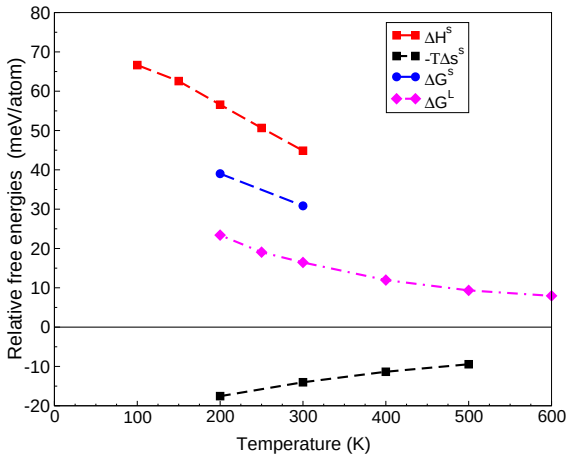

FIG. 2: Quantum corrections to various free energy terms at 50 GPa. Here $\Delta H^s = H^s_{qm} - H^l_{cl}$, $\Delta S^s = S^s_{qm} - S^l_{cl}$, and $\Delta G^s = G^s_{qm} - G^l_{cl}$ are the quantum corrections to the $cI16$ crystal enthalpy, entropy and Gibbs free energies, respectively. ΔG^L is the quantum correction to the liquid Gibbs free energy computed using Eq. (2).

cellent; the slight underestimate of the melting temperatures at 40 and 60 GPa is to be expected considering that $cI16$ is not the preferred crystalline phase at these pressures. In addition, the error bars on the computed melting temperatures are 25 K. They are estimated by considering by how much the melting temperatures change (20-25 K) when the relative free energies of the solid and liquid phases are varied by 5 meV/atom. These uncertainties produce systematic errors and thus have little effect on the computed shift of the melting temperatures that results from quantum ion effects. Furthermore, we note that the harmonic frequencies scale as $1/\sqrt{m_i}$, which means that if ^{6}Li were considered instead of ^{7}Li, ΔH^S would increase by about 8% or 4 meV/atom near the melting curve minimum (see Fig. 2). At the same time, ΔG^L, which scales as $1/m_i$, would be larger as well, by $\sim$ 3.2 meV/atom. The net isotope effect is thus smaller than about 1 meV/atom. Finally, we have determined[32] the Lindemann ratio, which at 50 GPa and 200 K is 0.20. This is indeed a noticeably large value and characteristic for the melting of a quantum solid.

The melting curve of Li is extended to higher compression by evaluating the melting temperatures of the *oC24* phase[8] in the pressure range from 100 to 175 GPa. The procedure for quantum ions described above was also followed here as well, with the only differences being that 96-atom supercells were used for the FPMD simulations of *oC24* and vibrational density of states obtained from the FPMD were used to calculate entropies. The latter ensures that anharmonic effects, which become more significant at elevated temperatures, are included in the computed free energies.

We have also used the empirical Simon law[34], which assumes no minimum, to fit the low pressure experimental

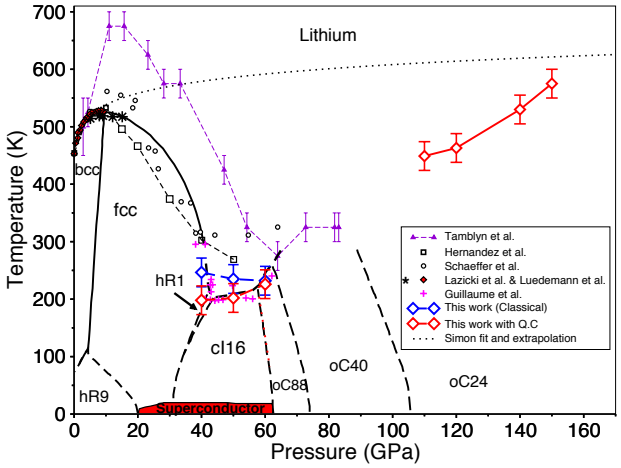

FIG. 3: Melting curve and phase diagram of dense Li. Melting temperatures obtained in this study with (shown in red) and without (blue) quantum corrections are compared with available experimental data[8,14,16,33] and previous theoretical results[5,13]. The dotted line is the extrapolation of the melting curve with the Simon law.

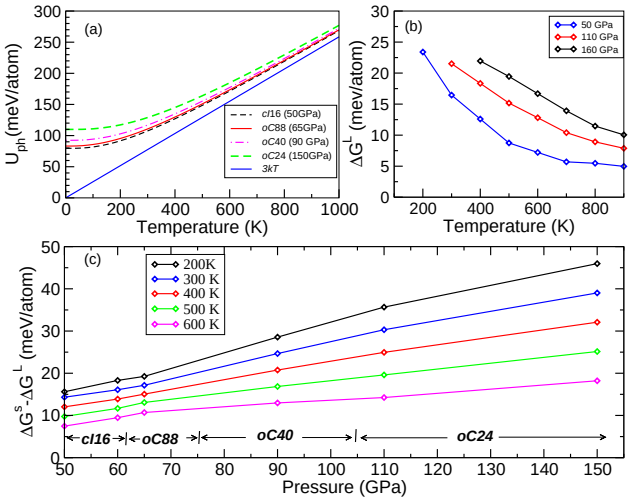

FIG. 4: (a) Phonon internal energies as a function of temperature for several Li structures, at pressures shown in the figure legend and compared with the classical 3kT dependence. (b) Quantum corrections to the liquid free energy as a function of temperature for three different pressures. (c) Difference between the quantum corrections of the solid and liquid phases as a function of pressure along several isotherms.

data and extrapolate the P-T melting points into the stability field of *oC24* (see Fig. 3) as no melting minimum exists. By comparing the extrapolation and the calculated at $P > 150$ GPa data points, it becomes clear that the Li melting curve resumes a positive slope once the solid transforms away from very complex phases. It is interesting to note that there are common features, such as deep melting minima, clustering of several complex solid phases, and resumption of positive melting curve, exhibited in the phase diagrams of the lighter alkalis: Li (see Fig. 3), Na (see Fig. 7 in Ref.[35]) and K (see Fig. 3 in Ref. [36]).

Note that even though the *oC* and *cI*16 space group symmetries are open structures compared to *fcc*, they are more dense because of *s*-to-*p* charge transfer. Our result for the melting curve above 100 GPa confirms the explanation[5] that the anomalous melting of Li is a consequence of parallel structural and electronic transitions taking place in the liquid and solid phases. They are analogous in both phases - symmetry breaking transitions driven by *s*-to-*p* charge transfer- but take place gradually in the liquid, and commence at lower pressure there in than in the solid.

Given the above analyis and parallel with the phase diagrams of other alkalis, a relevant question is whether a second region of anomalous melting at higher pressure may exist; a second melting minimum is known for Cs[37] and Rb[38]. Indeed, Tamblyn *et al.*[5] predicted that overlap of the Li 1*s* electrons at pressures above 150 GPa will ensue, by ∼350 GPa, in the emergence of a liquid with average tetrahedral local order. Quantum effects increase with compression and if the Li melting curve has a turnover above ∼ 200 GPa comparable to that observed below 50 GPa, proper consideration of quantum dynamics then becomes essential. Nevertheless, our results up to 150 GPa can be extrapolated in order to obtain an estimate for the magnitude of the quantum corrections at higher compressions.

Quantum corrections to the Gibbs free energies of liquid and solid Li for several isotherms from 50 to 150 GPa are shown in Fig. 4. The corrections for the liquid phase, ΔG^L, are calculated using Eq. (2). Those for the solid phase, ΔG^S, are estimated by taking the difference between the phonon internal energy, U_{ph}, and $3kT$ for the relevant structures reported reported by Guillaume *et al.*[8]. While the zero point energies vary among the different structures by as much as 30 meV/atom (Fig. 4 (a)), the differences become negligible by 500 K. As can be seen from the figure, the difference $\Delta G^S - \Delta G^L$ increases almost linearly with pressure for a fixed temperature. Thus the curves in Fig. 4 (c) can be extrapolated to estimate the magnitude of quantum corrections at higher pressure. For example, if the melting temperature of Li at 350 GPa is anticipated to be around 400 K, quantum effects would be responsible for changing the relative free energies of the solid and liquid phases by about 100 meV. The effect of such a change on the melting temperature will depend on the exact forms of the free energy curves as a function of temperature. Given the predicted[5] similarity of the tetrahedral local order of solid and liquid pases above 350 GPa, it is reasonable to assume that their free energies have similar temperature dependences as well. Therefore, a quantum correction of the order of 100 meV per atom may have a significant effect on the melting curve at these pressures. The possibility for a

low-temperature liquid Li at extreme compression is an intriguing question worth further study.

As a concluding comment we should note that though considerable care has been devoted to the calculations of all terms appearing in the Gibbs energy, it is clear that those of electronic origin (of major importance) are ultimately dependent on provisions of pseudopotentials, which as a matter of construction do not describe correctly charge densities in regions close to nuclei. Given the large density gradients in these regions, the importance of pseudopotential and exchange approximations may merit further scrutiny for a low atomic number system (with large zero-point motion), such as lithium, at extreme densities.

This work was supported by NSERC, LLNL, and the NSF (DMR 0907425/NWA). Computational resources were provided by Accent and WestGrid. We thank Brian Boats and Amanuel Teweldeberhan for technical help and discussions. S.A.B. performed work at LLNL under the auspices of the US Department of Energy under contract No. DE-AC52-07NA27344.

* Electronic address:bonev@llnl.gov

[1] J. Neaton and N. Ashcroft, Nature **400**, 141 (1999).
[2] M. Hanfland, K. Syassen, and N. Christensen, Nature **408**, 174 (2000).
[3] K. Shimizu, H. Ishikawa, D. Takao, T. Yagi, and K. Amaya, Nature **419**, 597 (2002).
[4] S. Deemyad and J. S. Schilling, Physical Review Letters **91**, 167001 (2003).
[5] I. Tamblyn, J.-Y. Raty, and S. A. Bonev, Physical Review Letters **101**, 075703 (2008).
[6] T. Matsuoka and K. Shimizu, Nature **458**, 186 (2009).
[7] T. Matsuoka, M. Sakata, Y. Nakamoto, K. Takahama, K. Ichimaru, K. Mukai, K. Ohta, N. Hirao, Y. Ohishi, and K. Shimizu, Physical Review B **89**, 144103 (2014).
[8] C. L. Guillaume, E. Gregoryanz, O. Degtyareva, M. I. McMahon, M. Hanfland, S. Evans, M. Guthrie, S. Sinogeikin, and H.-K. Mao, Nature Physics **7**, 211 (2011).
[9] J.-Y. Raty, E. Schwegler, and S. A. Bonev, Nature **449**, 448 (2007).
[10] E. Gregoryanz, O. Degtyareva, M. Somayazulu, R. J. Hemley, and H. K. Mao, Physical Review Letters **94**, 185502 (2005).
[11] H. E. and I. J., Physical Review Letters **98**, 055501 (2007).
[12] H. Eshet, R. Z. Khaliullin, T. D. Kuhne, J. Behler, and M. Parrinello, Physical Review Letters **108**, 115701 (2012).
[13] E. R. Hernández, A. Rodriguez-Prieto, A. Bergara, and D. Alfè, Phys. Rev. Lett. **104**, 185701 (2010).
[14] A. Lazicki and Y. Fei, Solid State Communications **150**, 625 (2010).
[15] F. A. Gorelli, S. F. Elatresh, C. L. Guillaume, M. Marqués, G. J. Ackland, M. Santoro, S. A. Bonev, and E. Gregoryanz, Physical Review Letters **108**, 055501 (2012).
[16] A. M. J. Schaeffer, W. B. Talmadge, S. R. Temple, and S. Deemyad, Physical Review Letters **109**, 185702 (2012).
[17] W. Kohn and L. Sham, Phys.Rev. **140**, A1133 (1965).
[18] J. P. Perdew, K. Burke, and M. Ernzerhof, Physical Review Letters **77**, 3865 (1996).
[19] G. Kresse and J. Hafner, Physical Review B **47**, 558 (1993).
[20] X. Gonze, Phys. Rev. B **55**, 10337 (1997).
[21] X. Gonze, B. Amadon, P. M. Anglade, J. M. Beuken, F. Bottin, P. Boulanger, F. Bruneval, D. Caliste, R. Caracas, M. Côté, et al., Computer Physics Communications **180**, 2582 (2009).
[22] C. Hartwigsen, S. Goedecker, and J. Hutter, arXiv.org **cond-mat.soft** (1998).
[23] P. Souvatzis, O. Eriksson, M. I. Katsnelson, and S. P. Rudin, Phys. Rev. Lett. **100**, 095901 (2008).
[24] A. M. Teweldeberhan and S. A. Bonev, Physical Review B **83**, 134120 (2011).
[25] P. Loubeyre and J. P. Hansen, Physics Letters **80A**, 181 (1980).
[26] P. Loubeyre, J. M. Besson, J. P. Pinceaux, and J. P. Hansen, Physical Review Letters **49**, 1172 (1982).
[27] P. Loubeyre, R. Letoullec, and J. P. Pinceaux, Physical Review Letters **69**, 1216 (1992).
[28] M. Boninsegni, C. Pierleoni, and D. M. Ceperley, Physical Review Letters **72**, 1854 (1994).
[29] L. Caillabet, S. Mazevet, and P. Loubeyre, Physical Review B **83**, 094101 (2011).
[30] V. Diatschenko, C. W. Chu, D. H. Liebenberg, D. A. Young, M. Ross, and R. L. Mills, Physical Review B **32**, 381 (1985).
[31] H. Y. Geng, R. Hoffmann, and Q. Wu, Physical Review B **92**, 104103 (2015).
[32] The Lindemann ratio is defined as $\sqrt{\langle u^2\rangle}/a$, where $\langle u^2\rangle$ is the mean square displacement of the atoms, and a is the nearest neighbor Li-Li distance. For Li in the $cI16$ structure at pressure 50 GPa, $a = 2.066$ Å. We calculate $\langle u^2\rangle$ by integrating the vibrational density of states, $g(\omega)$, according to $\langle u^2\rangle = \int d\omega g(\omega) \coth(\beta\hbar\omega/2)\frac{\hbar}{2m\omega}$, with normalization condition $\int d\omega g(\omega) = 1$. The value of $\sqrt{\langle u^2\rangle}$ at 50 GPa and 0 K is 0.290 Å, and at 200 K it is 0.412 Å.
[33] H. D. Luedemann and G. C. Kennedy, Journal of Geophysical Research **73**, 2795 (1968).
[34] E. Simon and G. Z. G. Z. Glatzel, Z. Anorg. Allg. Chem. **178**, 309 (1929).
[35] M. Marqués, M. Santoro, C. L. Guillaume, F. A. Gorelli, J. Contreras-Garcia, R. T. Howie, A. F. Goncharov, and E. Gregoryanz, Physical Review B **83**, 184106 (2011).
[36] O. Narygina, E. E. McBride, G. W. Stinton, and M. I. McMahon, Physical Review B **84**, 054111 (2011).
[37] A. Jayaraman, R. Newton, and J. McDonough, Phys. Rev. **159**, 527 (1967).
[38] R. Boehler and C.-S. Zha, Physica B+C **139-140**, 233 (1967).